1997PASP..109..827B

Publications of the Astronomical Society of the Pacific
109: 827–836, 1997 July

MANIAC: A New Mid- and Near-Infrared Array Camera

T. BÖKER[1]

Max-Planck-Institut für extraterrestrische Physik, Giessenbachstrasse, D-85740 Garching, Germany
Electronic mail: boeker@stsci.edu

J. W. V. STOREY

School of Physics, University of New South Wales, Sydney NSW 2052, Australia
Electronic mail: jwvs@newt.phys.unsw.edu.au

A. KRABBE

Max-Planck-Institut für extraterrestrische Physik, Giessenbachstrasse, D-85740 Garching, Germany
Electronic mail: krabbe@mpe-garching.mpg.de

T. LEHMANN

Universitäts-Sternwarte Jena, Schillergässchen 2, D-07745 Jena, Germany
Electronic mail: lehmi@astro.uni-jena.de

Received 1996 December 20; accepted 1997 March 12

ABSTRACT. We present the optical, mechanical and electronical design of MANIAC, the Mid- and Near-Infrared Array Camera, together with some results from the first observing run. MANIAC is a two-channel instrument that offers observations from 1 to 5 μm and from 8 to 28 μm at the same time. The advantages of the purely reflective optical design of MANIAC are discussed as well as the options that are provided by simultaneous observations in the two regimes. The construction of MANIAC will be completed in a modular way, each of the five phases offering a fully operational instrument. The first phase, a mid-infrared camera based on a Rockwell 128×128 pixel Si:As detector, has now been completed. With a pixel scale of about 0.2 arcsec, the MANIAC mid-infrared channel offers diffraction-limited imaging in the N and Q bands at a 4-m class telescope and a field of view of 26×26 arcsec. The sensitivity achieved in the N band is very close to the background limit under all observational modes. We also discuss the scientific importance of high-resolution mid-infrared observations, describe the observing methods, and characterize the performance of the detector array.

1. INTRODUCTION

The scientific importance of high-resolution observations in the atmospheric windows from 1 to 23 μm has been greatly increased by the successful launch of the *ISO* satellite. The high spectral resolution and sensitivity of *ISO* has already led to many interesting discoveries, that require follow-up observations with the high spatial resolution of modern ground-based telescopes. An 8-m class telescope, for example, could achieve sub-arcsec resolution for wavelengths all the way out to 30 μm—essential for the detailed understanding of many sources from planetary disks to galactic nuclei.

This is one of the major motivations behind the development of a single ground-based instrument that covers this whole spectral region. At the present time there is no detector that can offer good sensitivity over the full 1–23 μm range, and so we have adopted a dual-channel system. MANIAC, the Mid- And Near-Infrared Array Camera built at the Max-Planck-Institut für extraterrestrische Physik (MPE), is designed for simultaneous observations in the near-infrared (hereafter NIR) from 1 to 5 μm and the mid-infrared (MIR) from 8 to 28 μm. This dual-channel approach offers a number of unique features:

(1) perfect registration between NIR and MIR channels;
(2) the NIR images can generate shift vectors, either to drive a tip-tilt mirror or for shift-and-add routines in offline processing of the MIR data;
(3) modular construction, upgradeable in steps;
(4) straightforward upgrade path to future larger arrays to increase the field of view.

Other features of MANIAC include:

(a) broad- and narrow-band imaging with various filters;
(b) high-resolution spectroscopy with cryogenic Fabry–Perot in the MIR-channel;
(c) diffraction disk fully sampled for ultimate spatial resolution. For example, the pixelscale is 0.″2 at a 4-m class telescope, in comparison to the diffraction limit of 0.″6 at 10 μm;
(d) fully reflective optics in both channels, hence maximum throughput and achromatic performance over the whole spectral range;
(e) optional imaging polarimetry.

[1]Currently at: Space Telescope Science Institute, 3700 San Martin Drive, Baltimore, MD 21218

© 1997. Astronomical Society of the Pacific

© Astronomical Society of the Pacific • Provided by the NASA Astrophysics Data System

1997PASP..109..827B

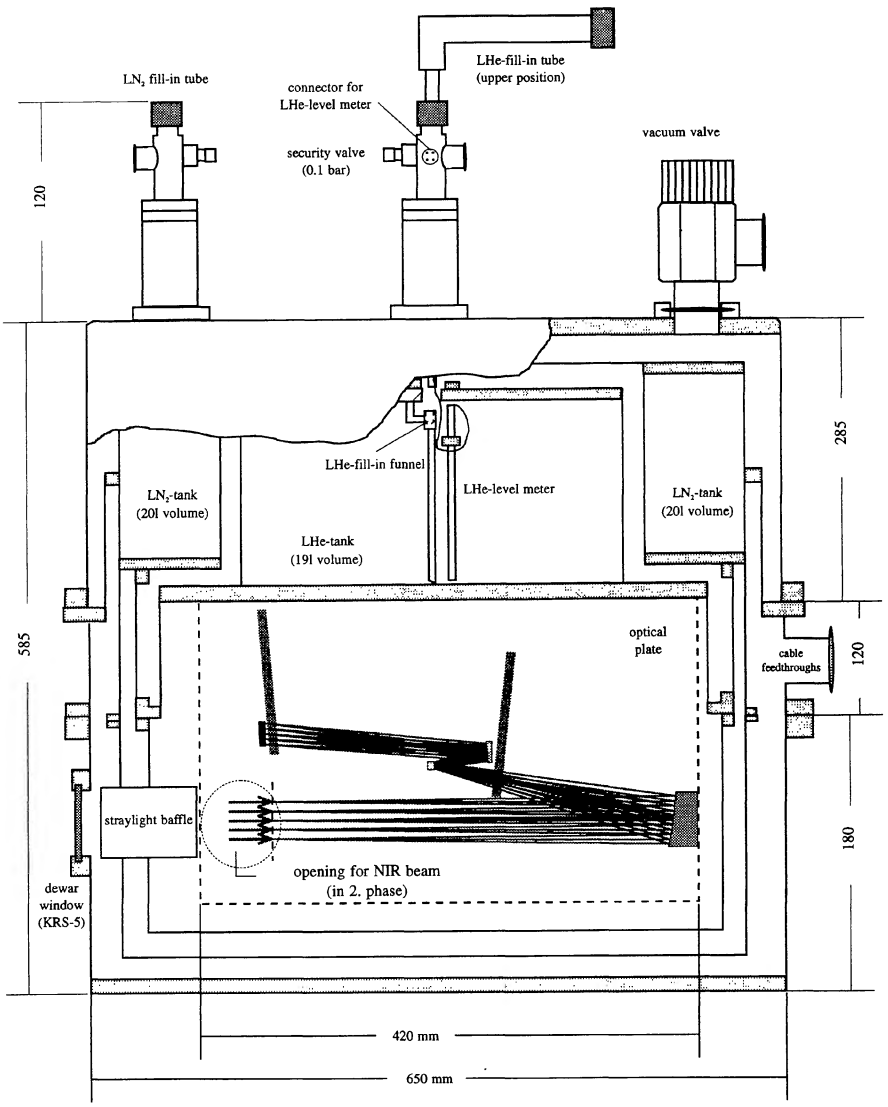

FIG. 1—Mechanical construction of the MANIAC cryostat. The optical plate is mounted "edge-on" to the helium tank; the MIR optics are shown on the front. All measures are in mm.

1.1 A Phased Approach

To minimize the technical risks, MANIAC has been designed to be built in stages. While each stage offers a fully functioning instrument, provision has been made for all future extensions. The single phases are:

(1) MIR camera based on a 128×128 pixel Si:As detector from Rockwell International, Anaheim, CA, USA. Fixed broad- and narrow-band filters are provided, together with a circular variable filter (CVF) for low-resolution spectroscopy;
(2) NIR camera based on a 256×256 pixel HgCdTe (NICMOS III) or similar array with fixed broad- and narrow-band filters;
(3) integration of a cryogenic Fabry–Perot into the MIR path;
(4) increase of the NIR field-of-view by changing the detector to a 512×512 pixel array;
(5) increase of the MIR field-of-view by changing the detector to a 256×256 pixel array.

In this paper, we report on the completion of the first phase of MANIAC. In the next section, we discuss the design of the camera, including the cryostat, all other mechanical components, and the optics. The MANIAC control system with the detector, the read-out electronics, and the computer control is described in Sec. 3. Section 4 describes the performance of the MIR channel of MANIAC. We conclude with some of the results from the first observing run in 1996 March at the ESO 2.2-m telescope at La Silla, Chile in Sec. 5.

2. THE DESIGN OF MANIAC

2.1 Mechanical Layout

Because of the strong emission of room-temperature blackbodies at MIR wavelengths, efficient cooling of all

© Astronomical Society of the Pacific • Provided by the NASA Astrophysics Data System

1997PASP..109..827B

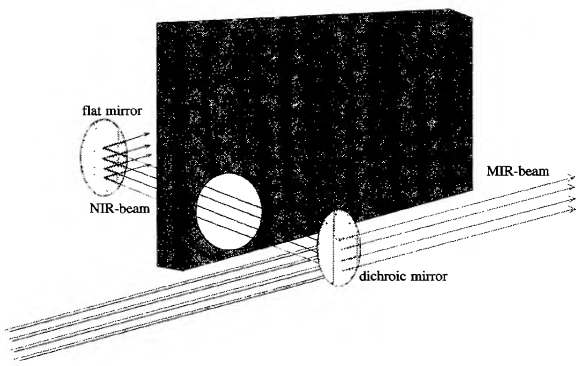

FIG. 2—Principle of the beamsplitting in MANIAC.

optical components to cryogenic temperatures is essential. In MANIAC, cooling is provided by a cylindrical cryostat with two 20 l tanks for liquid nitrogen and liquid helium. Figure 1 shows a schematic of the dewar. The optical baseplate is mounted "edge-on" on the liquid–helium tank. Both sides of the baseplate are used, one for each of the two channels. All optical parts of both channels (detectors, filters, mirrors, and Fabry–Perot) are at 4.2 K. The beam is split just before the telescope focal plane by a dichroic mirror as shown in Fig. 2. While the MIR part passes through the dichroic, the NIR part is reflected through a hole in the baseplate on the other side, where it is fed through the NIR camera optics. The layout of the MIR optics is shown in Fig. 3. The two filter wheels are driven by stepper motors mounted outside of the dewar; their movements are transmitted via ferrofluidic feedthroughs in the dewar wall. All mechanical and electrical feedthroughs are led through the middle ring of the cryostat, allowing easy access to the optics without needing to remove cables or mechanical feedthroughs.

The hold time of the filled helium tank with MANIAC in operation is currently 35 h. The total weight of the instrument is about 100 kg.

2.2 Optics

Because of the wide range of wavelengths covered by each of MANIAC's two channels, it would be difficult (though not impossible) to assure sufficiently good image quality over the whole MIR regime with a lens-based system. In addition to the usual lateral chromatic aberrations, lens-based systems frequently suffer from longitudinal chromatic aberration, requiring re-focusing of the system whenever the filter is changed. The purely reflective optical design of MANIAC is intrinsically achromatic over the whole wavelength range while still providing a layout compact enough to fit into a transportable, self-contained instrument.

2.2.1 The Mirrors

The optical layout is basically a reflecting analog of the "collimator-camera" design used in many refracting instruments. Referring to Fig. 3, the first mirror M1 is an off-axis paraboloid that creates an image of the telescope secondary mirror right at the second (spherical) mirror M2—which thus acts as the aperture stop of the system. Creating a good quality image here is important for efficient baffling to reduce the stray light. The diameter of M2 is 6 mm, chosen such that the divergence of the beam is sufficiently low that filters with the highest possible resolution ($R \approx 200$) can be

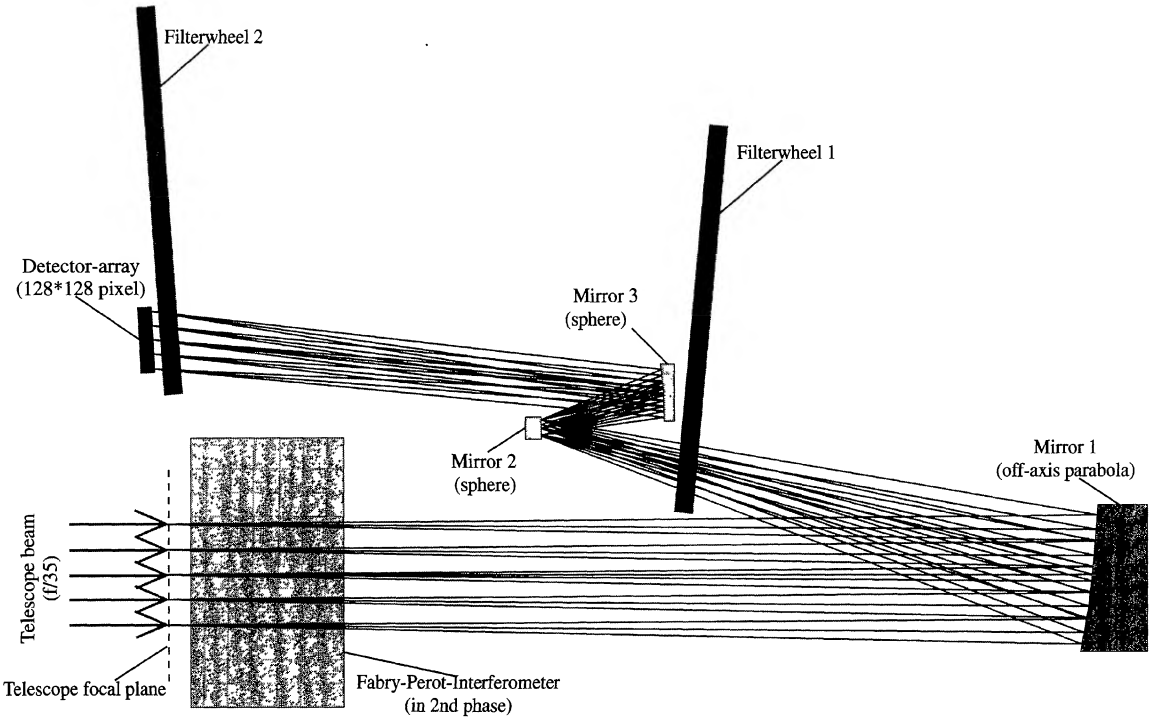

FIG. 3—Schematic of the MANIAC mid-infrared channel.

© Astronomical Society of the Pacific • Provided by the NASA Astrophysics Data System

1997PASP..109..827B

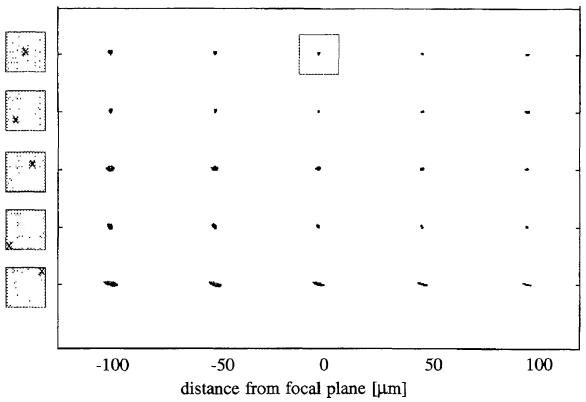

FIG. 4—MANIAC spot diagrams of various object points. Their position in the field-of-view is indicated on the left, its size is 51.″2 along one side (for a 256×256 pixel array in later phases). All aberrations (except distortion, see text) are much smaller than one pixel, the size of which is shown in the top row. The five columns are for different detector positions with respect to the nominal focal plane (i.e., different focus positions).

used without degradation in the first filter wheel in front of M2. The pupil diameter of 6 mm requires that the focal length of M1 be about 200 mm, which thus determines the overall size of the optics. A third mirror M3 (also spherical) folds the light through a second filter wheel onto the detector. Mirrors M2 and M3 form the "camera" section of the instrument; a wide range of magnifications is possible by a suitable selection of these two mirrors. The vertices of all three mirrors lie on a common axis which is offset 70 mm from the incoming beam. Such a system is called a *ring field* because the accessible field of view is an anulus approximately 1′ wide and with a radius of 70 mm.

Because the beam passing through the first filter wheel is very close to a pupil and is in excess of 6 mm diameter, it is not possible to place a CVF in this position without seriously degrading both its resolution and transmission. Instead, the CVF is placed in the second filter wheel immediately in front of the detector. A disadvantage of this location is that, at any given setting of the CVF, not all detector pixels see the same transmitted wavelength. However, the full resolution of the CVF is achieved and, by scanning the CVF through a few resolution elements, a "data cube" can be built up for subsequent off-line analysis.

The optical design has been optimized with the SIGMA59 software package from Kidger Optics Ltd., Crowborough, England. Figure 4 shows the spot diagrams of various points in the field of view at different detector offsets from the nominal focal plane. The optimization has already been done for the larger detector arrays in future stages of MANIAC, therefore the field of view in Fig. 4 is twice as large as for the 128×128 array.

Clearly, all aberrations are negligible, with the important exception of distortion. Distortion, which is not displayed in this kind of a spot diagram, causes a variation in plate scale across the image. At the extreme corners of the MANIAC field of view, all object points are still imaged with a spot size much smaller than one pixel, but offset from their nominal positions by roughly 2%. However, because the distortion in MANIAC is the same for all wavelengths and absolutely stable, it can be easily corrected for during the off-line data analysis.

TABLE 1
Mirror Data

Mirror	Type	Clear Diam. (mm)	Curv. Radius (mm)	Vertex Pos. (mm)
M1	off-axis parabola	62.20	400.00	340.21 to tel. focal plane
M2	sphere	6.01	−123.18	203.48 to M1
M3	sphere	23.80	148.34	45.00 to M2
Detector	flat	9.6×9.6	···	185.96 to M3

Table 1 summarizes the sizes, curvatures, and positions of all three mirrors after optimisation. They were diamond turned at INTOP, Frickingen, Germany from AlMg4.5Mn, an alloy with favorable mechanical and cryogenic properties. This is the same material as that of the baseplate, thus providing homologous contraction during cooldown. Some details of the mechanical challenges in achieving the necessary high precision can be found in Langenbeck (1992). An interesting feature of the MANIAC optics is that the mirrors and their sockets are machined in one piece. This reduces the number of degrees of freedom and thus dramatically simplifies the adjustment procedure. To account for the critical positioning and adjustment of the mirrors (the optical design showed that acceptable tolerances are about 100 μm in displacement along the beam and 3′ in tilt), steel pins were put in the baseplate and positioned on the common optical axis of all three mirrors. Thus not only are the relative distances fixed to high accuracy, but in addition the alignment of the tilts is made very straightforward. The mirrors are adjusted to be parallel by using a laser in autocollimation on the reflective, high-quality backside surface of the mirrors. To ensure optimum reflectivity, the mirror surfaces have been gold coated. Figure 5 shows a photograph of the mirror system.

2.2.2 *Window and Filters*

The MANIAC entrance window is made from 8 mm thick KRS-5, with an anti-reflection coating that covers the

FIG. 5—Photograph of the MANIAC mirror system.

© Astronomical Society of the Pacific • Provided by the NASA Astrophysics Data System

1997PASP..109..827B

TABLE 2
Filter Data

Filter	$\lambda_{central}$ (μm)	$\Delta\lambda$ (μm)	T_{max} (%)
N-band	10.50	5.0	80
Q′-band	17.60	1.80	60
Q-band	20.00	5.40	45
"Sweet Spot"	8.03	0.15	45
continuum	10.36	0.12	60
S IV	10.53	0.12	60
continuum	10.68	0.12	60
continuum	12.56	0.15	54
Ne II	12.82	0.15	54
continuum	12.95	0.12	62
continuum	18.43	0.19	40
S III	18.73	0.19	40
continuum	19.00	0.21	40
CVF	7.7–14.0	R ≈ 60	70

wavelength range from 1 and 28 μm. The MIR camera of MANIAC has a total of 13 broad- and narrow-band filters in two filter wheels. Table 2 gives an overview of their central wavelengths, widths, and maximum transmissions. All filters are 1 in. diameter, on a germanium substrate. Since the number of optical coating layers on a single filter is limited, blocking up to 30 μm is provided by a second germanium substrate attached to the actual filter. All filters were produced by International Research and Development, Newcastle upon Tyne, England, and measured at cryogenic temperatures at MPE.

3. DATA ACQUISITION SYSTEM

3.1 Detector

The MIR camera of MANIAC is built around a Rockwell (128×128) pixel Si:As array. Table 3 summarizes the performance of the array. The numbers are taken from the Rockwell test report and were fully confirmed during our laboratory tests with MANIAC.

TABLE 3
Detector Data

Quantity	Value
Size	(128×128) Pixel
Pixel size	(75×75) μm
Good pixels	99.94%
Number of outputs	4
Operating temperature	≤ 12 K
Active layer thickness	15 μm
Active layer doping density	1×10^{18}cm^{-3}
Well capacity[a]	8.5×10^{6}
Read noise	590 e^-
Det. quantum efficiency[b]	0.21
Dark current	≤ 5e^-

[a]Signal value with 10% deviation from ideal curve.
[b]Detective quantum efficiency η/β.

Notes to TABLE 3

All numbers are taken from the Rockwell test report. Measurements were performed under the following conditions: detector bias 1.5 V, temperature 5 K, wavelength 10.6 μm, frametime 98.3 ms, signal 10^{12} photons/s. Our laboratory tests agree with the test report.

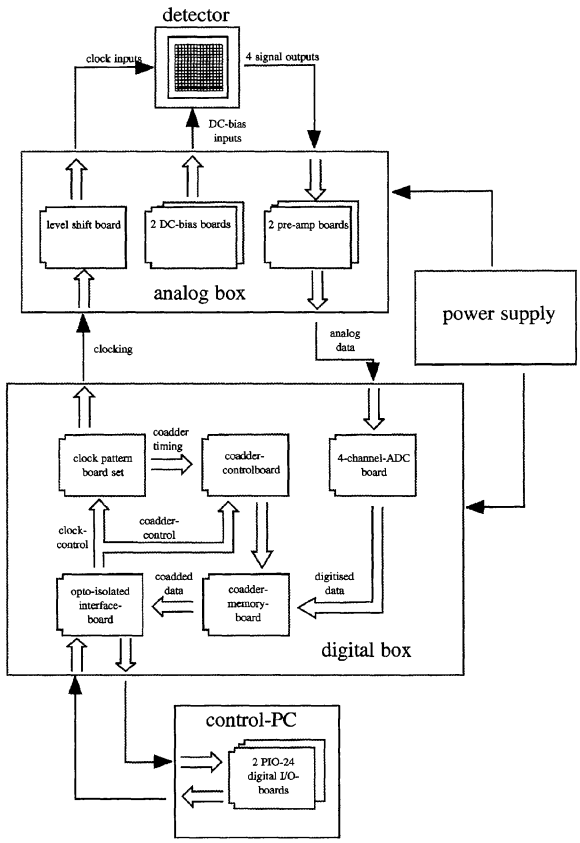

FIG. 6—Schematic of the MANIAC read-out electronics.

3.2 Read-out Modes

The available read-out modes of the Rockwell array are single read (SR) and a mode that, for want of a better name, has become known as uncorrelated double sampling (UDS). In UDS, the detector is reset twice prior to the beginning of each integration. However, the multiplexer design allows the reset level to be sampled only after the *first* of these resets. Correlating the output signal with the first reset eliminates $1/f$ noise in the preamplifier, but does nothing to reduce kTC noise (in fact, it increases by $\sqrt{2}$). However, with a detector operating temperature of 4.2 K and a node capacitance of 2.1 pF, the kTC noise is in any case negligible at 70 rms electrons. Newer versions of the multiplexer also allow correlated double sampling (CDS) and higher order modes. During the MANIAC observations, we normally used UDS to reduce the $1/f$ noise; however for broadband imaging in the N and Q band we had to use the faster SR to avoid saturation, which otherwise would occur even at the fastest read-out speed of 400 frames s^{-1}.

3.3 Read-out Electronics

When operating the broadband at MIR wavelengths, some 4×10^9 photons per second are falling on each detector pixel (for a 4-m telescope and 0.2-arcsec pixels). Given a well depth of 1×10^7 electrons and an assumed instrument transmission of 25%, one immediately sees that the minimum read-out speed is 100 Hz. This means 100

© Astronomical Society of the Pacific • Provided by the NASA Astrophysics Data System

1997PASP..109..827B

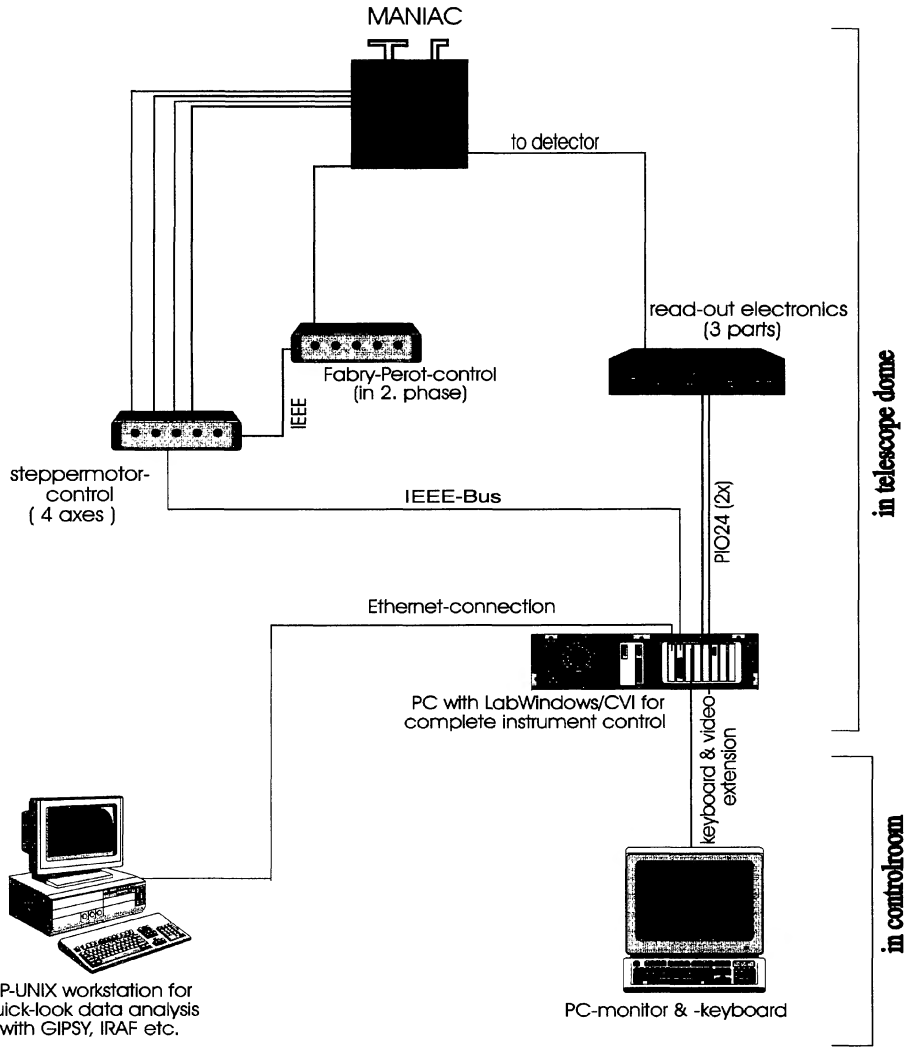

FIG. 7—MANIAC data-acquisition system.

$\times 128^2 = 1.6 \times 10^6$ pixel readouts per second, and when converting to 14-bit integers this corresponds to 2.9 Mbyte per second. Clearly, such data rates are beyond current microcomputer capabilities. One way out of this dilemma is to add up a number of data frames in a special "coadder" circuit before reading them into the PC, thus lowering the data rates.

The principle of the MANIAC read-out electronics is shown in Fig. 6. It consists of three separate boxes:

(a) An analog box, which reads in the four detector outputs and amplifies them. It also generates all detector biases and the clock signals for the array.
(b) A digital box for reading in the preamplified detector outputs from the analog box, digitizing and coadding them at up to 400 frames per second. It also communicates with the PC over two standard serial IO boards.
(c) A power supply for both boxes.

The data from the four detector outputs are led via shielded coaxial cables into the four low-noise preamplifiers with adjustable gain. The amplified data are led into the digital box, again via coaxial cables, to fast Analog-to-Digital Converters (ADCs). The digital data, which at this point still have the high rate of the pixel reads, are then summed in hardware coadder circuits until the PC calls them via an opto-isolated PIO-24 link.

In the opposite direction, the user commands entered into the PC are transferred again via a PIO-24 link to the individual boards like the clock generator or coadder controller. The clock generator provides the TTL signals for the timing of the level shift board in the analog box, where the correct bias levels for reading out the detector array are produced. All other (constant) detector biases are also generated adjustable in the analog box and fed via a separate cable bundle to the array.

The complete system was built by Wallace Instruments in Ithaca, NY, USA.

3.4 Computer Control System

A multipurpose instrument like MANIAC requires an ability to adapt rapidly to a multitude of observing condi-

© Astronomical Society of the Pacific • Provided by the NASA Astrophysics Data System

1997PASP..109..827B

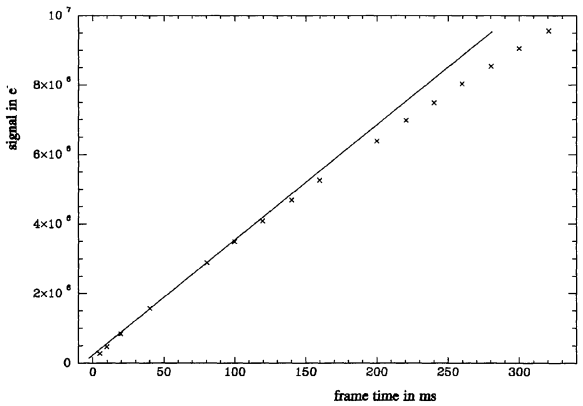

FIG. 8—Linearity of the Rockwell Si:As array measured during laboratory tests at MPE. The 10% deviation from the ideal curve (solid line) occurs at approximately $8\times10^6e^-$.

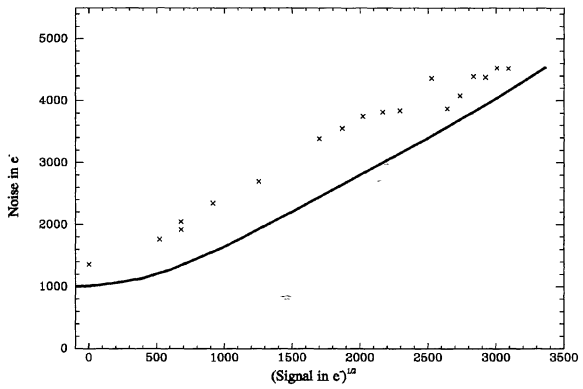

FIG. 9—Noise measurements for various signal levels. The solid line is the theoretical noise limit.

tions. Besides the control of the filter wheels, the data acquisition system (DAS) must be able to select various read-out modes of the detector and the parameters of the observation such as integration time and read-out speed. In the case of MANIAC, this task is done by a single IBM-compatible PC running under Microsoft Windows. It operates the read-out electronics, records the data from it, displays the data on the screen, and stores them onto the disk. Simultaneously, it provides full control of all movable parts. The PC runs LabWindows/CVI, a package from National Instruments that allows creation of graphical user surfaces that can be used as virtual instruments. Figure 7 shows a schematic of the MANIAC DAS. The PC, together with the read-out electronics, sits in a standard 19 in. rack at the Cassegrain focus of the telescope. The only connection to the control room is via a video and keyboard extension and an ethernet link for data transfer.

4. PERFORMANCE OF MANIAC

To verify the performance of the optics, the detector and the read-out electronics, extensive tests were done both in the laboratory and during the first run at the telescope which are described in detail in Böker (1996). This section summarizes the most important results.

4.1 Linearity

Figure 8 shows the detector output versus integration time for a constant flux level. A 10% deviation of the output from the ideal (solid) line occurs roughly at $8\times10^6e^-$; this is usually defined as the well depth of the array. The number is in agreement with that from the Rockwell test report.

4.2 Noise

Noise measurements were performed for various signal levels using a temperature adjustable blackbody. Figure 9 shows the results of these measurements. The solid line is the theoretical noise limit, given by the expression $\sqrt{N_{\rm read}^2+N_{\rm ADC}^2+\beta\cdot N_{\rm stat}^2}$, where $N_{\rm read}$ is the detector read noise, $N_{\rm ADC}$ is the ADC noise (in the case of MANIAC, $N_{\rm read}\approx 600e^-$, and $N_{\rm ADC}\approx 700e^-$), and $N_{\rm stat}$ is the statistical shot noise. The factor β is the gain dispersion, given by $\langle G^2\rangle/\langle G\rangle^2$, where G is the detector gain. For this detector, $\beta\approx 1.3$. Our results are consistent with the quoted detective quantum efficiency of $\eta/\beta\approx 0.21$.

The measured excess noise in the MANIAC electronics is in the range of 1.3–1.6 and does not significantly reduce the sensitivity. We are confident that as we gain experience with the system, this excess will be reduced even further.

4.3 Point-Spread Function

The imaging quality of the MANIAC mirror optics was verified during the commissioning nights at the 2.2-m telescope. Figure 10 shows two images of the M3.5 III star γ Cru, on the left in the N band and on the right in the Q band. In both images the first Airy rings are clearly visible, demonstrating that diffraction-limited performance has been achieved.

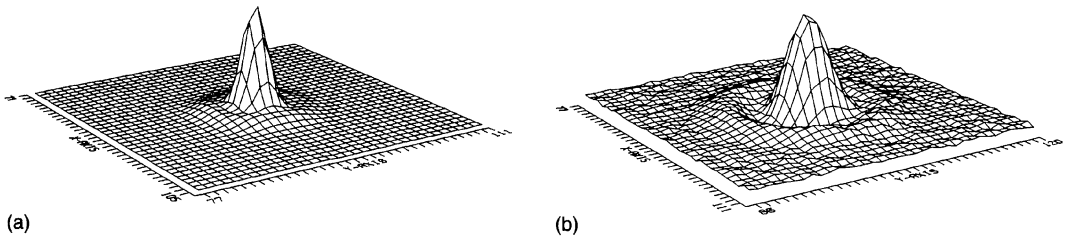

FIG. 10—Point-spread function of MANIAC. The star observed was γCru, the filters used were N band (left) and Q band (right), and the integration time was 3 min for each image. Clearly visible in both images are the first Airy rings, demonstrating diffraction-limited performance.

© Astronomical Society of the Pacific • Provided by the NASA Astrophysics Data System

1997PASP..109..827B

TABLE 4
MANIAC MIR-channel Performance

Quantity	Value
Wavelength range	8–28 μm
f-ratio	f/35
Pixel scale[b]	0.″345
Field of view[b]	(44.″2×44.″2)
Instrumenttransmission[a]	11%
N-band NEP[b,c]	1.7 mJy pixel^{-1}, 1σ, 1 h

[a]Incl. atmosphere, telescope, window, mirrors, filter, and detector.
[b]Numbers refer to operation at the ESO 2.2-m telescope.
[c]Value achieved at the first observing run, it refers to the described on-chip chop-nod observing technique and is limited by the humid atmosphere and the dusty telescope primary mirror during that period.

4.4 Summary of the MANIAC Performance

Table 4 summarizes the performance of the MANIAC MIR channel at its first run from 1996 March 5–10 at the ESO 2.2-m telescope at La Silla. The sensitivity achieved during this run was limited by the very humid atmosphere and the dusty telescope primary mirror. Nevertheless, as shown in Table 5, MANIAC is already competitive with other MIR cameras; this is also demonstrated by some of the first scientific results presented in the next section.

5. FIRST RESULTS

One of the major motivations for the development of MANIAC was the possibility of obtaining both line and continuum images of the nuclei of external galaxies at arcsec resolution. To demonstrate MANIAC's ability to perform this kind of research, we present here two examples from the first run, namely NGC 3256 and NGC 1808.

TABLE 5
Comparison to other MIR-Cameras

Instrument	Location	Detector	NEP	Ref.
MIRACLE	MPE	SBRC 58×62 Si:As	1.24	1
MIRAC	Univ. of Arizona	Hughes 20×64 Si:As	0.12	2
SpectroCam-10	Cornell Univ.	Rockwell 128×128 Si:As	0.34	3
Timmi	ESO	Leti/LIR 64×64 Si:Ga	0.64	4
MANIAC	MPE	Rockwell 128×128 Si:As	0.41	

Notes to TABLE 5

All NEP's are in Jy/□″ and refer to 1σ in 1 sec on-source integration time with a 10% filter at a 3-m telescope. References: (1) Cameron et al. 1992; (2) Hoffmann et al. 1993; (3) Hayward et al. 1993; (4) Käufl et al. 1994.

5.1 Observing Technique

Due to the highly variable sky background, fast chopping at a minimum frequency of 3 Hz was necessary during the whole run. We chopped in the East–West direction. Because the different secondary positions caused different emission patterns of the telescope structure, the result image of the on–off subtraction still has residuals in it that are much stronger than the object itself. We therefore nodded the telescope approximately every 5 min in the North–South direction and repeated the chopping process. Subtracting the on–off images of both nod positions then removes almost all residuals.

For sufficiently compact objects both chop and nod amplitude were small enough to leave the object on the detector, so that 100% observing efficiency was obtained. This is the favored mode of observation and hereafter is called the "on-chip chop-nod" technique.

5.2 NGC 3256

NGC 3256 is a well-known merger system at a distance of 56 Mpc. The structure of the prominent tidal tails indi-

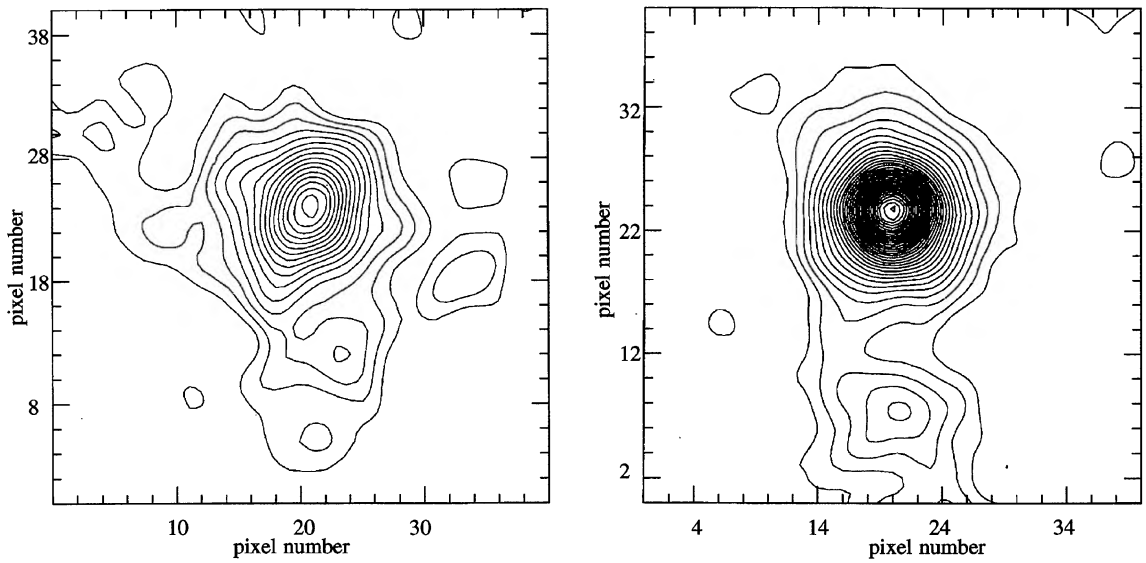

FIG. 11—MANIAC maps of NGC 3256. Left: [Ne II] (+ continuum), right: N band. The field of view shown is 13.″8 in both cases (0.″345 per pixel), the integration time was 80 (24) min for [Ne II] (N band). The resolution is approximately 1.″5 (diffraction limit at 12.8 μm at a 2.2-m telescope). North is up and West is to the left. The double nucleus is clearly visible in both images. Contour levels (in arbitrary units) are linear and range from 1.6 to 18.2 in steps of 0.52 for the N band and 1.48–9.73 in steps of 0.55 for the [Ne II] map.

© Astronomical Society of the Pacific • Provided by the NASA Astrophysics Data System

1997PASP..109..827B

FIG. 12—Comparison of the MANIAC [Ne II] (+continuum) map in color with the 6 cm radio-continuum map of Norris and Forbes (1995) in contours.

cates the merging of two spirals with comparable masses (Toomre and Toomre 1972). With a total luminosity (8–1000 μm) of $3\times10^{11}\ L_{\odot}$ (Sargent et al. 1989), NGC 3256 is the most luminous galaxy with a redshift below 3000 km s^{-1}.

The strong and extended 10 μm emission, half of which originates outside the central kpc, is important evidence for star-formation activity (Graham et al. 1984; Joseph and Wright 1985). Other evidence that the extreme bolometric luminosity is caused by a recent episode of vigorous star formation comes from the prominent PAH emission features (Moorwood 1986) and the deep CO bandheads at 2.3 μm (Doyon et al. 1994). A detailed spectroscopic study with the ISO-SWS has recently shown that the stars that ionize their surroundings have temperatures around 40,000 K, indicative of a burst with an age of a few Myrs (Rigopolou et al. 1996).

We observed NGC 3256 during two nights in the N band and in the [Ne II] emission line filter at 12.81 μm. Figure 11 shows both maps in a contour representation. The on-source integration time was 80 min (24 min) for the [Ne II] (N band) image. The resolution is about 1.″5 (diffraction limit at 12.8 μm at the 2.2-m telescope). Both maps were obtained in an on-chip chop-nod mode. They both clearly show two components of emission, however the secondary peak in the [Ne II] map is slightly offset from that in the N-band map. Note that no continuum was subtracted from the [Ne II] image. This is likely to explain the elongated structure of the primary [Ne II] peak. The comparison with the Hα map of Moorwood and Oliva (1994) shows that the [Ne II]-emission, which should agree with the Hα, indeed has a similar morphology, given our somewhat coarser resolution.

In Fig. 12 we compare the [Ne II] map to the 6 cm radio map of Norris and Forbes (1995). Despite the lower signal-to-noise ratio of the former, there is very good agreement between the two images. The different brightness ratios between the two peaks might indicate variations in the extinction towards the two nuclei.

5.3 NGC 1808

The nearby (D = 11 Mpc) peculiar (type Sbc pec) spiral NGC 1808 is a well-studied example of a "hot-spot" galaxy that shows many signs of vigorous star formation. The central $\approx$ 750 pc in particular contains a number of bright compact ($\approx 1''$) NIR emission knots (Krabbe et al. 1994, hereafter KSG 1994) interpreted as dense H II regions. In Fig. 13 we present the N-band map obtained with MANIAC, together with the line map of the Brγ emission

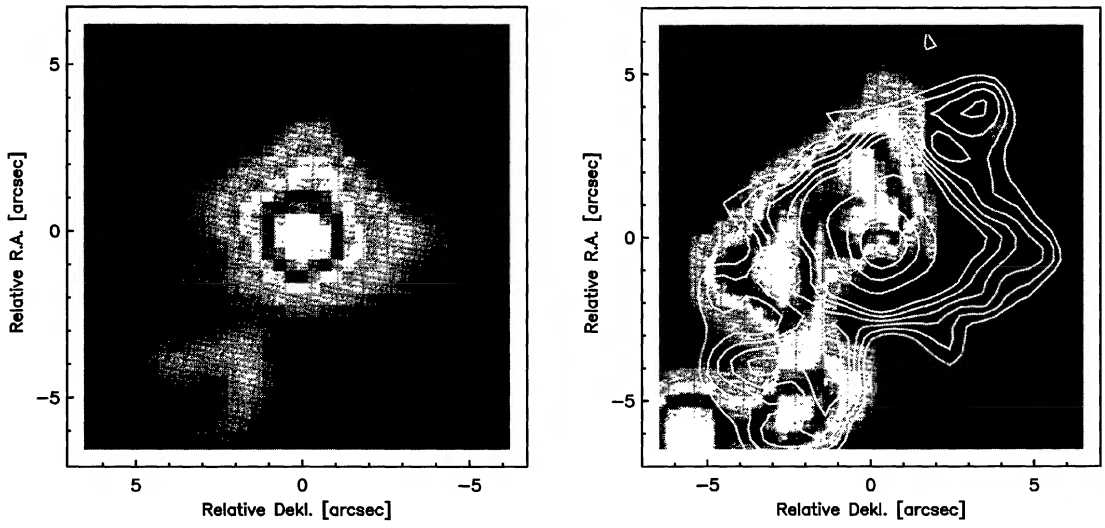

FIG. 13—Left: MANIAC N-band map of NGC 1808 with a resolution of 1.″1. Right: Brγ map from Krabbe et al. (1994) in color compared to the MANIAC N-band map in contours.

© Astronomical Society of the Pacific • Provided by the NASA Astrophysics Data System

1997PASP..109..827B

taken from KSG 1994. Total integration time for this map was 21 min; we again used an on-chip chop-nod technique.

For this comparison, we positioned the MIR centroid on the K-band centroid of KSG 1994. The overall agreement between the maps is fairly good to the east of the centroids, suggesting that in these regions the MIR emission is due to warm dust heated to several hundred K by the UV radiation of the young stars in the Brγ knots. To the west of the nucleus, however, no Brγ emission is observed, while the MIR shows a more symmetric distribution which is also seen in the coarser map by Telesco et al. (1993). Our interpretation is that the interstellar medium is optically thick for Brγ emission, but not for MIR radiation. The NIR emission which is also symmetric to the nucleus as seen in the K-band map of KSG 1994 is dominated by the light of the more evolved and cooler giants of type around K5 or later which presumably are not confined to the dense H II regions where the extinction is high.

6. SUMMARY

We have reported on the completion of phase one of MANIAC, a new camera system for simultaneous observations in the NIR and MIR. This first phase, a mid-IR camera, has been described and the overall performance characterized. The camera's sensitivity is very close to the background limit, and first results from a run at the ESO 2.2-m telescope in March 1996 are very encouraging. Completion of the next stage of MANIAC, the NIR channel, is scheduled for 1997.

We wish to thank the ESO staff at La Silla for their help in making the commissioning run a success. In particular, we are grateful to Ueli Weilenmann and Hans Gemperlein for their support of "Los Maniacos." We also thank Gerd Jakob for his help in preparing the run at MPE, Russell Wallace for his continuous support, and Richard A. Florence at Rockwell International for allowing us to publish data from their test report. J.W.V.S. thanks the Alexander von Humboldt Foundation and the Australian Department of Industry Science and Tourism (sic) for their support.

REFERENCES

Böker, T. 1996, Ph.D. thesis, Max-Planck-Institut für extraterrestrische Physik, Garching, Germany
Cameron, M., Storey, J. W. V., Rotaciuc, V., Genzel, R., Drapatz, S., Krabbe, A., Verstraete, L., and Lee, T. 1992, ESO Proc., 42, 705
Doyon, R., Joseph, R. D., and Wright, G. S. 1994, ApJ, 421, 101
Graham, J. R., Wright, G. S., Meikle, W. P. S., Joseph, R. D., and Bodee, M. F. 1984, Nature, 310, 2313
Hayward, T. L., Miles, J. W., Houck, J. R., Gull, G. E., and Schoenwald, J. 1993, Proc. SPIE, 1946, 334
Hoffmann, W. F., Fazio, G. G., Shivanandan, K., Hora, J. L., and Deutsch, L. K. 1993, Proc. SPIE, 1946, 449
Joseph, R. D., and Wright, G. S. 1985, MNRAS, 214, 87
Käufl, H. U. et al. 1994, Infrared Phys. Technol., 35, 203
Krabbe, A., Sternberg, A., and Genzel, R. 1994, ApJ, 425, 72
Langenbeck, P. 1992, Precision Eng. 14, 43
Moorwood, A. F. M. 1986, A&A, 166, 4
Norris, R. P., and Forbes, D. A. 1995, ApJ, 446, 594
Moorwood, A. F. M., and Oliva, E. 1994, ApJ, 429, 602
Rigopoulou, D. et al. 1996, A&A (in press)
Sargent, A. I., Sanders, D. B., and Phillips, T. G. 1989, ApJ, 346, L9
Telesco, C. M., Dressel, L. L., and Wolstencroft, R. D. 1993, ApJ, 414, 120
Toomre, A., and Toomre, J. 1972, ApJ, 286, L79

© Astronomical Society of the Pacific • Provided by the NASA Astrophysics Data System